

Retrolensing by a charged black hole

Naoki Tsukamoto* and Yungui Gong†

School of Physics, Huazhong University of Science and Technology, Wuhan 430074, China

Abstract

Compact objects with a light sphere such as black holes and wormholes can reflect light rays like a mirror. This gravitational lensing phenomenon is called retrolensing and it is an interesting tool to survey dark and compact objects with a light sphere near the solar system. In this paper, we calculate the deflection angle in the strong deflection limit analytically in the Reissner-Nordström spacetime without the expansion in power of the electrical charge. Using the obtained deflection angle in the strong deflection limit, we investigate a retrolensing light curve and the separation of a double image by the light sphere of a Reissner-Nordström black hole.

* tsukamoto@rikkyo.ac.jp

† yggong@mail.hust.edu.cn

I. INTRODUCTION

Gravitational lensing is an important phenomenon to survey dark and compact objects and to confirm gravitational theories from a solar system scale to a cosmological scale. Gravitational lensing has been investigated mainly under a quasi-Newtonian approximation or a weak-field approximation [1–4] but gravitational lensing over the quasi-Newtonian approximation also has been studied [5, 6]. Darwin pointed out that faint images near the circular orbit of a light ray called light sphere or photon sphere [7, 8] appear in the Schwarzschild spacetime in 1959 [9] and the gravitational lensing phenomena have been revived several times [10–24]. The gravitational lensing by a light sphere in various black hole [17, 25–52], naked singularity [17, 53–55], and wormhole spacetimes [18, 55–60] has been also investigated.

Recently, LIGO has reported a gravitational-wave event GW150914 [61] and it has shown the existence of heavy stellar-mass black holes with the mass $M \geq 25M_{\odot}$ in nature [62]. Black holes are becoming an important target in astronomy and astrophysics and gravitational lensing by black holes will be an important tool to research dim and isolated black holes.

Holz and Wheeler [63] proposed to survey retrolensing caused by sun lights which reflected by a light sphere of a stellar-mass black hole near the solar system in 2002. A black hole in Galactic center as a retrolens [64–66], wormholes as retrolenses [59], and the effect of the rotation [65, 67] and the electrical charge [64] of a black hole on the magnification were also studied. In Ref. [17], Bozza considered gravitational lensing effects of light rays passed near a light sphere in a general static and spherical symmetric spacetime and provided a formula of the deflection angle in a strong deflection limit. The deflection angle in the strong deflection limit describes a fundamental feature of a light sphere and the relations between the deflection angle in the strong deflection limit and the quasinormal modes [68, 69] and the high-energy absorption cross section [70] were also discussed. Eiroa and Torres [64] and Bozza and Mancini [65] showed that the deflection angle in the strong deflection limit is useful to obtain retrolensing light curves in the general static and spherical symmetric spacetime.

Considering the difference of observables between a Schwarzschild black hole and the other black holes is important to check whether a observed non-rotating black hole really can be

described by the Schwarzschild black hole. The Reissner-Nordström black hole solution is one of useful and simple black hole solutions for the purpose even though black holes in nature would be almost electrically neutralized. The deflection angle in the strong deflection limit in the Reissner-Nordström black hole spacetime has been obtained numerically by Eiroa *et al.* in Ref. [26]. Bozza investigated the deflection angle in the strong deflection limit in the Reissner-Nordström black hole spacetime and pointed out an integral in the deflection angle cannot be calculated analytically in Ref. [17]. The integral was calculated numerically and the expansion of the integral in power of the electrical charge was calculated analytically [17].

In this paper, we revisit the deflection angle in the strong deflection angle in the Reissner-Nordström spacetime and investigate the effect of the electrical charge on retrolensing light curves and the separation of a double image. We revise a strong deflection limit analysis investigated by Bozza [17] to obtain the deflection angle in the strong deflection limit in the Reissner-Nordström black hole spacetime analytically.

This paper is organized as follows. In Sec. II we investigate the deflection angle in the strong deflection limit in the Reissner-Nordström spacetime and obtain it analytically without the expansion in power of an electrical charge. In Sec. III we review retrolensing and investigate the effect of an electrical charge on retrolensing light curves and a double image by a retrolens in the Reissner-Nordström spacetime. In Sec. IV we conclude our results. In this paper we use the units in which the light speed and Newton's constant are unity.

II. DEFLECTION ANGLE IN THE STRONG DEFLECTION LIMIT IN THE REISSNER-NORDSTRÖM SPACETIME

In this section, we calculate the deflection angle α of a light ray in a strong deflection limit in the Reissner-Nordström spacetime in a following form:

$$\alpha(b) = -\bar{a} \log \left(\frac{b}{b_c} - 1 \right) + \bar{b} + O((b - b_c) \log(b - b_c)), \quad (2.1)$$

where b is the impact parameter of the light ray, b_c is the critical impact parameter of the light ray, \bar{a} is a positive function of Q/M which is the ratio of the electrical charge Q to the Arnowitt-Deser-Misner mass M of a Reissner-Nordström black hole, and \bar{b} is a function of

Q/M .¹ The line element in the Reissner-Nordström spacetime is given by

$$ds^2 = -\frac{\Delta(r)}{r^2}dt^2 + \frac{r^2}{\Delta(r)}dr^2 + r^2(d\theta^2 + \sin^2\theta d\phi^2), \quad (2.2)$$

where $\Delta(r) = r^2 - 2Mr + Q^2$. There are time translational and axial Killing vectors $t^\mu\partial_\mu = \partial_t$ and $\phi^\mu\partial_\mu = \partial_\phi$ because the spacetime is a static and spherical symmetric spacetime, respectively. If $Q \leq M$ is satisfied, an event horizon exists at $r = r_H$, where

$$r_H \equiv M + \sqrt{M^2 - Q^2}. \quad (2.3)$$

Please note that $r = r_H$ is the largest positive solution of the equation $\Delta(r) = 0$. We concentrate on the black hole spacetime. A light sphere exists at $r = r_m$, where r_m is given by

$$r_m = \frac{3M + \sqrt{9M^2 - 8Q^2}}{2}. \quad (2.4)$$

The radius of the light sphere r_m is the largest positive solution of an equation [8]

$$\frac{g'_{\theta\theta}(r)}{g_{\theta\theta}(r)} - \frac{g'_{tt}(r)}{g_{tt}(r)} = 0, \quad (2.5)$$

where $'$ is the differentiation with respect to the radial coordinate r . Note that

$$r_m^2 - 3Mr_m + 2Q^2 = 0. \quad (2.6)$$

The trajectory of a light ray is described by

$$k^\mu k_\mu = 0, \quad (2.7)$$

where $k^\mu \equiv \dot{x}^\mu$ is the wave number of the light ray and the dot denotes the differentiation with respect to an affine parameter parameterizing the null geodesic. The conserved energy E and angular momentum L of the photon given by

$$E \equiv -g_{\mu\nu}t^\mu k^\nu = \frac{\Delta(r)}{r^2}\dot{t} \quad (2.8)$$

and

$$L \equiv g_{\mu\nu}\phi^\mu k^\nu = r^2\dot{\phi}, \quad (2.9)$$

¹ In [17], the order of an error term in the deflection angle in the strong deflection limit is estimated as $O(b - b_c)$. Recently, however, Tsukamoto pointed out that the order of the error term should be read as $O((b - b_c)\log(b - b_c))$. See Ref. [59] for the details.

respectively, are constant along the null geodesic. We assume that E is positive. We define the impact parameter b of a light ray as

$$b \equiv \frac{L}{E} = \frac{r^4 \dot{\phi}}{\Delta(r) \dot{t}}. \quad (2.10)$$

We can assume L and b are positive without loss of generality as long as we consider one light ray. We assume $\theta = \pi/2$ without loss of generality.

From Eq. (2.7), the trajectory equation in the Reissner-Nordström spacetime is given by

$$-\frac{\Delta}{r^2} \dot{t}^2 + \frac{r^2}{\Delta} \dot{r}^2 + r^2 \dot{\phi}^2 = 0 \quad (2.11)$$

and it is expressed as

$$\dot{r}^2 = V(r), \quad (2.12)$$

where $V(r)$ is the effective potential for the motion of the photon defined as

$$V(r) \equiv E^2 - \frac{\Delta(r)}{r^4} L^2. \quad (2.13)$$

The motion of the photon is permitted in a region where $V(r)$ is non-negative. Since the effective potential $V(r)$ in the limit $r \rightarrow \infty$ becomes

$$V(r) \rightarrow E^2 > 0, \quad (2.14)$$

a photon can exist at $r \rightarrow \infty$. We consider that a photon comes from infinity, is reflected by a black hole at the closest distance $r = r_0$, and goes to infinity. Since \dot{r} vanishes at the closest distance $r = r_0$, from Eqs. (2.12) and (2.13), we obtain a relation between the impact parameter b and the closest distance r_0 as

$$b(r_0) = \frac{r_0^2}{\sqrt{\Delta_0}}, \quad (2.15)$$

where $\Delta_0 \equiv \Delta(r_0)$. Hereafter subscript 0 denotes the quantities at the closest distance $r = r_0$.

We define the critical impact parameter b_c as

$$b_c(r_m) \equiv \lim_{r_0 \rightarrow r_m} b(r_0) = \lim_{r_0 \rightarrow r_m} \frac{r_0^2}{\sqrt{\Delta(r_0)}}. \quad (2.16)$$

We call the limit $r_0 \rightarrow r_m$ or $b \rightarrow b_c$ strong deflection limit. The impact parameter $b(r_0)$ can be expanded in power of $r_0 - r_m$ as

$$\begin{aligned} b(r_0) &= b_c(r_m) + \frac{3Mr_m - 4Q^2}{2(Mr_m - Q^2)^{\frac{3}{2}}} (r_0 - r_m)^2 \\ &\quad + O((r_0 - r_m)^3). \end{aligned} \quad (2.17)$$

From the derivative of the effective potential $V(r)$ with respect to the radial coordinate r given by

$$V'(r) = \frac{2L(r^2 - 3Mr + 2Q^2)}{r^5} \quad (2.18)$$

and Eqs. (2.6) and (2.12), we obtain

$$\lim_{r_0 \rightarrow r_m} V(r_0) = 0 \quad (2.19)$$

and

$$\lim_{r_0 \rightarrow r_m} V'(r_0) = 0. \quad (2.20)$$

Thus, in the strong deflection limit $r_0 \rightarrow r_m$ or $b \rightarrow b_c$, a photon with the impact parameter $b \rightarrow b_c$ almost stops in the radial direction near outside the light sphere at $r = r_m$ and the orbit of the photon winds around the light sphere.

The trajectory equation (2.11) can be rewritten as

$$\left(\frac{dr}{d\phi}\right)^2 = r^4 \left(\frac{1}{b^2} - \frac{\Delta}{r^4}\right) \quad (2.21)$$

and then the deflection angle $\alpha(r_0)$ of the light ray is obtained as

$$\alpha = I(r_0) - \pi, \quad (2.22)$$

where

$$I(r_0) \equiv 2 \int_{r_0}^{\infty} \frac{dr}{r^2 \sqrt{\frac{1}{b^2} - \frac{\Delta}{r^4}}}. \quad (2.23)$$

By introducing a variable z defined as ²

$$z \equiv 1 - \frac{r_0}{r}, \quad (2.25)$$

$I(r_0)$ can be rewritten as

$$I(r_0) = \int_0^1 f(z, r_0) dz, \quad (2.26)$$

where

$$f(z, r_0) \equiv \frac{2r_0}{\sqrt{c_1(r_0)z + c_2(r_0)z^2 + c_3(r_0)z^3 + c_4(r_0)z^4}}, \quad (2.27)$$

² In Ref. [17], Bozza introduced a variable $z_{[17]}$ defined by

$$z_{[17]} \equiv \frac{-g_{tt}(r) + g_{tt}(r_0)}{1 + g_{tt}(r_0)} \quad (2.24)$$

in our notation. See Eqs. (10) and (11) in [17]. The difference between z and $z_{[17]}$ is discussed in Sec. IV in this paper.

where

$$c_1(r_0) \equiv 2(r_0^2 - 3Mr_0 + 2Q^2), \quad (2.28)$$

$$c_2(r_0) \equiv -r_0^2 + 6Mr_0 - 6Q^2, \quad (2.29)$$

$$c_3(r_0) \equiv -2Mr_0 + 4Q^2, \quad (2.30)$$

and

$$c_4(r_0) \equiv -Q^2. \quad (2.31)$$

Since $c_1(r_0)$ and $c_2(r_0)$ in the strong deflection limit $r_0 \rightarrow r_m$ become

$$c_1(r_0) \rightarrow 0 \quad (2.32)$$

and

$$c_2(r_0) \rightarrow 3Mr_m - 4Q^2, \quad (2.33)$$

respectively, the order of the divergence of $f(z, r_0)$ is z^{-1} . We separate $I(r_0)$ into two parts, i.e., a divergent part $I_D(r_0)$ and a regular part $I_R(r_0)$: $I(r_0) = I_D(r_0) + I_R(r_0)$. The divergent part $I_D(r_0)$ is defined as

$$I_D(r_0) \equiv \int_0^1 f_D(z, r_0) dz, \quad (2.34)$$

where

$$f_D(z, r_0) \equiv \frac{2r_0}{\sqrt{c_1(r_0)z + c_2(r_0)z^2}}. \quad (2.35)$$

The divergent part $I_D(r_0)$ can be integrated and we obtain

$$\begin{aligned} I_D(r_0) = & \frac{4r_0}{\sqrt{-r_0^2 + 6Mr_0 - 6Q^2}} \\ & \times \log \frac{\sqrt{-r_0^2 + 6Mr_0 - 6Q^2} + \sqrt{r_0^2 - 2Q^2}}{\sqrt{2(r_0^2 - 3Mr_0 + 2Q^2)}}. \end{aligned} \quad (2.36)$$

Using Eq. (2.17), I_D in the strong deflection limit $r_0 \rightarrow r_m$ or $b \rightarrow b_c$ is expressed as

$$\begin{aligned} I_D(b) = & -\bar{a} \log \left(\frac{b}{b_c} - 1 \right) + \bar{a} \log \frac{2(3Mr_m - 4Q^2)}{Mr_m - Q^2} \\ & + O((b - b_c) \log(b - b_c)), \end{aligned} \quad (2.37)$$

where \bar{a} is given by

$$\bar{a} = \frac{r_m}{\sqrt{3Mr_m - 4Q^2}}. \quad (2.38)$$

One sees that \bar{a} is the factor in the deflection angle in the strong deflection limit (2.1) later.

The regular part I_R is defined by

$$I_R(r_0) \equiv \int_0^1 f_R(z, r_0) dz, \quad (2.39)$$

where

$$f_R(z, r_0) \equiv f(z, r_0) - f_D(z, r_0). \quad (2.40)$$

Since we are interested in the deflection angle in the strong deflection limit $r_0 \rightarrow r_m$, we consider

$$\begin{aligned} \lim_{r_0 \rightarrow r_m} f_R(z, r_0) &= \frac{2r_m}{z\sqrt{c_2(r_m) + c_3(r_m)z + c_4(r_m)z^2}} \\ &\quad - \frac{2r_m}{z\sqrt{c_2(r_m)}}. \end{aligned} \quad (2.41)$$

We can integrate $I_R(r_0)$ in the strong deflection limit $r_0 \rightarrow r_m$ or $b \rightarrow b_c$ analytically and obtain it as

$$\begin{aligned} I_R(b) &= \bar{a} \log \left[\frac{4(3Mr_m - 4Q^2)^2}{M^2 r_m^2 (Mr_m - Q^2)} \right. \\ &\quad \times \left. \left(2\sqrt{Mr_m - Q^2} - \sqrt{3Mr_m - 4Q^2} \right)^2 \right] \\ &\quad + O((b - b_c) \log(b - b_c)). \end{aligned} \quad (2.42)$$

Thus, the deflection angle $\alpha(b)$ in the strong deflection limit $b \rightarrow b_c$ is given by

$$\alpha(b) = -\bar{a} \log \left(\frac{b}{b_c} - 1 \right) + \bar{b} + O((b - b_c) \log(b - b_c)), \quad (2.43)$$

where \bar{a} and \bar{b} are obtained as

$$\bar{a} = \frac{r_m}{\sqrt{3Mr_m - 4Q^2}} \quad (2.44)$$

and

$$\begin{aligned} \bar{b} &= \bar{a} \log \left[\frac{8(3Mr_m - 4Q^2)^3}{M^2 r_m^2 (Mr_m - Q^2)^2} \right. \\ &\quad \times \left. \left(2\sqrt{Mr_m - Q^2} - \sqrt{3Mr_m - 4Q^2} \right)^2 \right] - \pi, \end{aligned} \quad (2.45)$$

respectively. Figure 1 shows b_c/M , r_m/M , \bar{a} , and \bar{b} as the functions of Q/M . When the black hole has no charge ($Q = 0$), we obtain $b_c = 3\sqrt{3}M$, $\bar{a} = 1$, and $\bar{b} = \log [216(7 - 4\sqrt{3})] - \pi$.

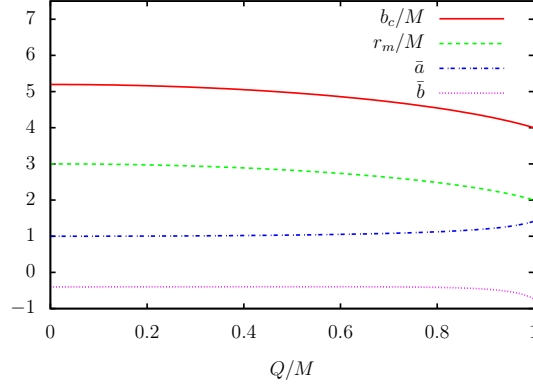


FIG. 1. Quantities in the Reissner-Nordström spacetime as the functions of Q/M . The (red) solid, (green) dashed, (blue) dash-dotted, and (purple) dotted curves denote b_c/M , r_m/M , \bar{a} , and \bar{b} , respectively.

They are equivalent to a well-known result in Refs. [9, 17] in the Schwarzschild spacetime. When the black hole has the maximal charge ($Q = M$), we obtain $b_c = 4M$, $\bar{a} = \sqrt{2}$, and $\bar{b} = 2\sqrt{2} \log [4(2 - \sqrt{2})] - \pi$.

In [17], \bar{a} in the Reissner-Nordström spacetime was obtained as, in our notation,

$$\bar{a} = \frac{r_m \sqrt{Mr_m - Q^2}}{\sqrt{M(6M - r_m)r_m^2 - 9r_mMQ^2 + 4Q^4}}. \quad (2.46)$$

Using Eq. (2.6), one shows that Eq. (2.46) is equivalent to Eq. (2.44).

III. RETROLENSING IN THE REISSNER-NORDSTRÖM SPACETIME

In this section, we review retrolensing following Ref. [65] and then we investigate retrolensing in the Reissner-Nordström spacetime.

A. Lens equation

We consider that the ray of the sun S is reflected by the light sphere L of a black hole with a deflection angle α and reaches an observer O . The observer sights an image I with an image angle θ . The lens configuration is shown in Fig. 2.

We solve a lens equation proposed by Ohanian [12, 22, 65],

$$\beta = \pi - \alpha(\theta) + \theta + \bar{\theta}, \quad (3.1)$$

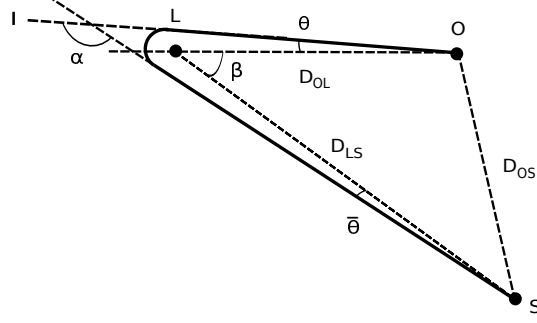


FIG. 2. Lens Configuration. The ray of the sun S is reflected by a light sphere L of a black hole with a deflection angle α and reaches an observer O . The observer sights an image I with an image angle θ . β is a source angle defined $\angle OLS$. $\bar{\theta}$ is an angle between a line LS and the light ray at S .

where β is a source angle $\angle OLS$ defined in a range $0 \leq \beta \leq \pi$ and $\bar{\theta}$ is an angle between a line LS and the light ray at S . We assume that the black hole, the observer, and the sun are almost aligned in this order. Under the assumption, we obtain

$$\beta \sim 0 \quad (3.2)$$

and

$$D_{LS} = D_{OL} + D_{OS}, \quad (3.3)$$

where D_{LS} , D_{OL} , and D_{OS} are the distances between the black hole and the sun, between the black hole and the observer, and between the observer and the sun, respectively. We concentrate on a case where the impact parameter b is positive and we assume that the radius of light sphere is much smaller than the distances between the black hole and the observer and between the black hole and the sun, i.e., $b_c \ll D_{OL}$ and $b_c \ll D_{LS}$.

B. Image angle and magnification

Neglecting the small terms $\theta = b/D_{OL}$ and $\bar{\theta} = b/D_{LS}$ in the Ohanian lens equation (3.1) and inserting the deflection angle $\alpha(b)$ in the strong deflection limit (2.43) and $b = \theta D_{OL}$ into the Ohanian lens equation (3.1), we obtain the positive solution $\theta = \theta_+(\beta)$ of the Ohanian lens equation as [65]

$$\theta_+(\beta) \equiv \theta_m \left[1 + \exp \left(\frac{\bar{b} - \pi + \beta}{\bar{a}} \right) \right], \quad (3.4)$$

where $\theta_m \equiv b_c/D_{OL}$ is the image angle of the light sphere of the black hole.

The magnification μ_+ of the image with the image angles θ_+ is given by [65]

$$\mu_+(\beta) = -\frac{D_{OS}^2}{D_{LS}^2} s(\beta) \theta_+ \frac{d\theta_+}{d\beta}, \quad (3.5)$$

where

$$s(\beta) = \frac{1}{\beta} \quad (3.6)$$

for a point source. We assume that the sun can be described by an uniform-luminous disk with a finite size on the observer's sky [71–73]. In an uniform-luminous and finite-size source case, $s(\beta)$ is given by an integral over the disk on the source plane,

$$s(\beta) = \frac{1}{\pi\beta_s^2} \int_{Disk} d\beta' d\phi, \quad (3.7)$$

where β' is a nondimensionalized radial coordinate divided by D_{LS} on the source plane, ϕ is the azimuthal coordinate around an origin on the source plane, $\beta_s \equiv R_s/D_{LS}$, and R_s is the radius of the sun. We fix an intersection point of the axis $\beta = 0$ and the source plane as the origin of the coordinates on the source plane and then $s(\beta)$ is expressed as

$$s(\beta) = \frac{2}{\pi\beta_s^2} \left[\pi(\beta_s - \beta) + \int_{-\beta+\beta_s}^{\beta+\beta_s} \arccos \frac{\beta^2 + \beta'^2 - \beta_s^2}{2\beta\beta'} d\beta' \right] \quad (3.8)$$

for $\beta \leq \beta_s$ and

$$s(\beta) = \frac{2}{\pi\beta_s^2} \int_{\beta-\beta_s}^{\beta+\beta_s} \arccos \frac{\beta^2 + \beta'^2 - \beta_s^2}{2\beta\beta'} d\beta' \quad (3.9)$$

for $\beta_s \leq \beta$. When the black hole, the observer and the sun are perfectly aligned, we obtain $s(\beta)$ as

$$s(0) = \frac{2}{\beta_s}. \quad (3.10)$$

From Eqs. (3.4) and (3.5), the magnifications $\mu_+(\beta)$ is given by [65]

$$\mu_+(\beta) = -\frac{D_{OS}^2}{D_{LS}^2} \frac{\theta_m^2 e^{(\bar{b}-\pi)/\bar{a}} \left[1 + e^{(\bar{b}-\pi)/\bar{a}} \right]}{\bar{a}} s(\beta). \quad (3.11)$$

A negative solution $\theta = \theta_-(\beta)$ of the Ohanian lens equation is given by

$$\theta_-(\beta) = -\theta_+(-\beta) \sim -\theta_+(\beta) \quad (3.12)$$

and its magnification $\mu_-(\beta)$ is obtained as

$$\mu_-(\beta) \sim -\mu_+(\beta) \quad (3.13)$$

because of spherical symmetry. The total magnification $\mu_{tot}(\beta)$ of the double image is given by

$$\begin{aligned} \mu_{tot}(\beta) &\equiv |\mu_+(\beta)| + |\mu_-(\beta)| \\ &= 2 \frac{D_{OS}^2}{D_{LS}^2} \frac{\theta_m^2 e^{(\bar{b}-\pi)/\bar{a}} \left[1 + e^{(\bar{b}-\pi)/\bar{a}} \right]}{\bar{a}} |s(\beta)|. \end{aligned} \quad (3.14)$$

The total magnification in a perfect-aligned case is obtained as

$$\mu_{tot}(0) = 4 \frac{D_{OS}^2}{D_{LS}^2} \frac{\theta_m^2 e^{(\bar{b}-\pi)/\bar{a}} \left[1 + e^{(\bar{b}-\pi)/\bar{a}} \right]}{\bar{a}\beta_s}. \quad (3.15)$$

C. Light curve

We consider retrolensing light curves by a black hole moving with the orbital velocity of the sun on the source plane with a distance $D_{OL} = 0.01\text{pc}$. See Fig. 3. We define β_{min} as

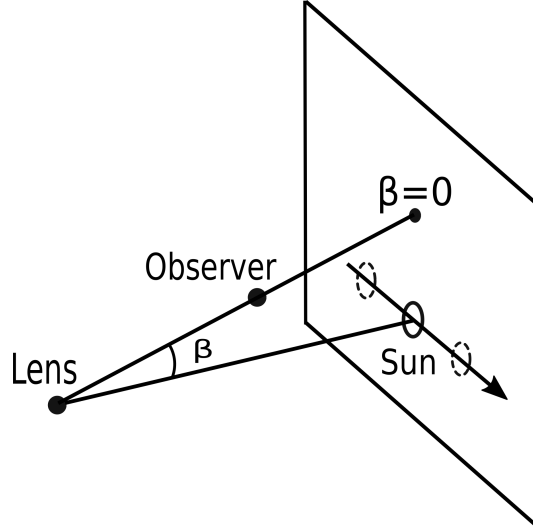


FIG. 3. The sun moves on the source plane with the orbital velocity of the sun.

the closest separation between the center of the sun disk and the axis $\beta = 0$ on the source plane. See Fig. 4 for the closest separation β_{min} . The light curves by a black hole with a

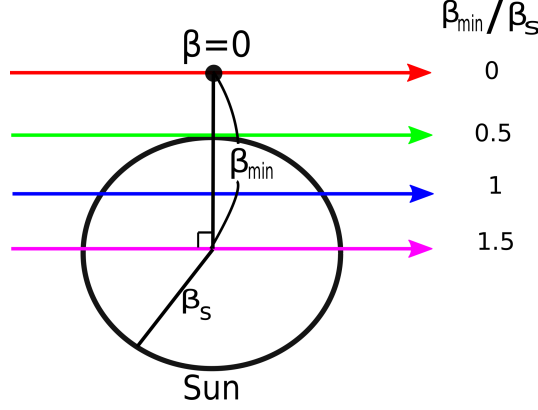


FIG. 4. The motion of the sun with the closest separation β_{min} between the center of the sun disk and the axis $\beta = 0$ on the source plane. The (red) first, (green) second, (blue) third, and (purple) fourth right arrows from top denotes the cases for $\beta_{min} = 0, 0.5\beta_s, \beta_s$, and $1.5\beta_s$, respectively.

mass $M = 10M_\odot$ and with a vanishing charge $Q = 0$ are shown in Fig. 5. We consider the cases for $\beta_{min} = 0, 0.5\beta_s, \beta_s$, and $1.5\beta_s$. The light curves show characteristic shapes

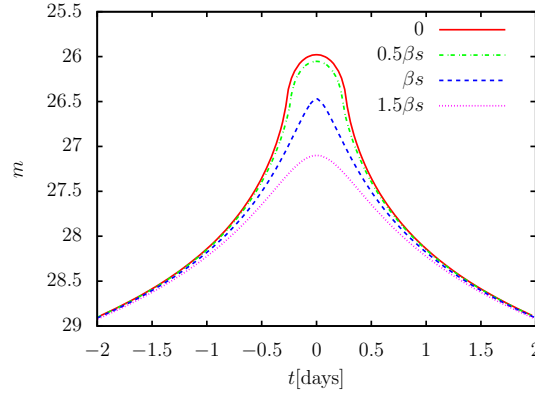


FIG. 5. Retrolensing light curves by a non-charged black hole with a mass $M = 10M_\odot$ at $D_{OL} = 0.01$ pc. The (red) solid, (green) dash-dotted, (blue) dashed, and (purple) dotted curves denote the light curves with the closest separation $\beta_{min} = 0, 0.5\beta_s, 1\beta_s$, and $1.5\beta_s$, respectively.

at the peak depending on a reduced closest separation β_{min}/β_s . From the shape of the peak, we would estimate the reduced closest separation β_{min}/β_s with an accuracy which be sufficient for following discussions. Please note also that the light curves do not diverge in the perfect-aligned case $\beta_{min} = 0$ and the peak magnitude is given by Eq. (3.15).

Figure 6 shows that retrolensing light curves reflected by a black hole with the mass

$M = 10M_\odot$, $30M_\odot$, and $60M_\odot$ with $Q = 0$ and at $D_{OL} = 0.01\text{pc}$ in the perfect-aligned case ($\beta_{min} = 0$). The light curves show clearly that the apparent brightness of the double image or its total magnification μ_{tot} is in proportion to M^2 . Figure 7 shows that two light curves

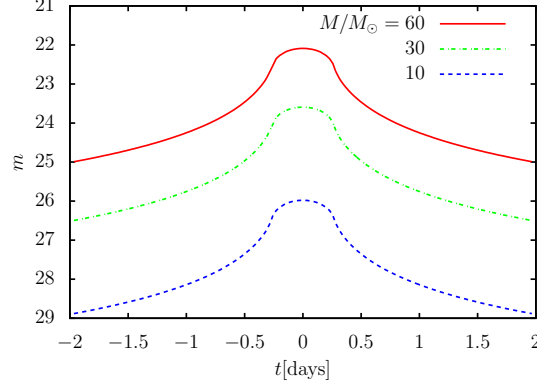


FIG. 6. Retrolensing light curves reflected by a non-charged black hole ($Q = 0$) at $D_{OL} = 0.01\text{pc}$ in the perfect-aligned case ($\beta_{min} = 0$). The (red) solid, (green) dash-dotted, and (blue) dashed curves denote the light curves lensed by a black hole with the mass $M = 60M_\odot$, $30M_\odot$, and $10M_\odot$, respectively.

by a black hole with the mass $M = 60M_\odot$ and with the electrical charge $Q = 0$ and $Q = M$ at $D_{OL} = 0.01\text{pc}$ in the perfect-aligned case ($\beta_{min} = 0$). We notice that the electrical charge of the black hole does not change the light curve much. The apparent magnitude m of the light curves at the peaks in the perfect-aligned case ($\beta_{min} = 0$) as a function of Q/M is shown in Fig. 8.

We consider the relative magnitude Δm of the peak of a light curve by a charged black hole with respect to the apparent magnitude of the one by a non-charged black hole with the same mass and position as the ones of the charged black hole. Figure 9 shows the relative magnitude Δm as a function of Q/M . The relative magnitude Δm for the black hole at $D_{OL} = 0.01\text{pc}$ with the mass $M = 60M_\odot$ in a perfect-aligned case is showed only in Fig. 9 but the ones with $M = 10M_\odot$ and $M = 30M_\odot$ are very similar to the one with $M = 60M_\odot$. From Figs. 1 and 9, we notice that the peak magnitude of the light curves does not change monotonically as the electrical charge Q increases while \bar{a} , \bar{b} , and $\theta_m = b_c/D_{OL}$ change monotonically. Fig. 1 shows that \bar{a} and \bar{b} monotonically increases and decreases, respectively, as the electrical charge Q increases. A factor in Eq. (3.15), $e^{(\bar{b}-\pi)/\bar{a}}$, increases and decreases

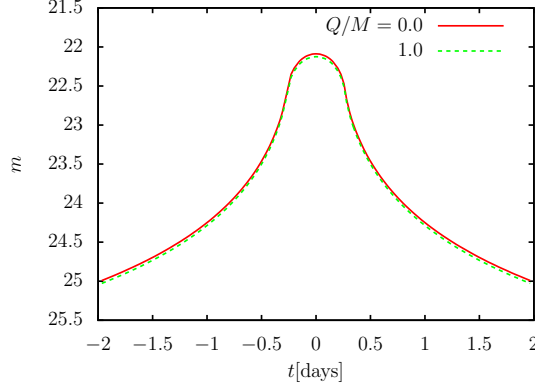


FIG. 7. Retrolensing light curves in the perfect-aligned case ($\beta_{min} = 0$) lensed by a black hole with the mass $M = 60M_{\odot}$ at $D_{OL} = 0.01\text{pc}$. The (red) solid and (green) dash-dotted curves denote the light curves lensed by the non-charged black hole ($Q = 0$) and the maximal charged black hole ($Q = M$), respectively.

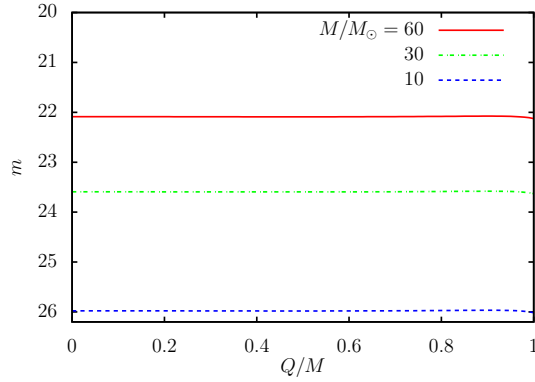


FIG. 8. The apparent magnitude m of the light curves at the peaks in the perfect-aligned case ($\beta_{min} = 0$) by a black hole at $D_{OL} = 0.01\text{pc}$ as a function of Q/M . The (red) solid, (green) dash-dotted, and (blue) dashed curves denote the apparent magnitude m of the peak of the light curves lensed by the black hole with the mass $M = 60M_{\odot}$, $30M_{\odot}$, and $10M_{\odot}$, respectively.

as \bar{a} increases and \bar{b} decreases, respectively. Thus, the non-monotonical behavior of the relative magnitude Δm is not surprising.

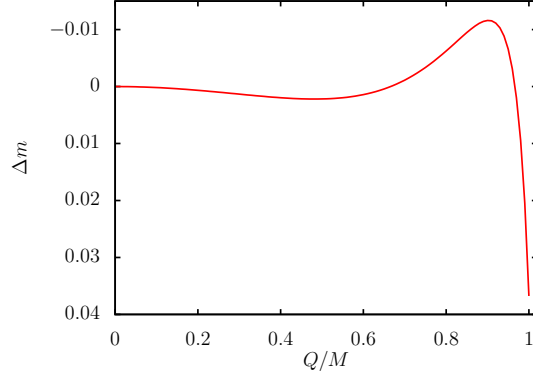


FIG. 9. Relative magnitude Δm by a black hole at $D_{OL} = 0.01\text{pc}$ in the perfect-aligned case ($\beta_{min} = 0$) as a function of Q/M . The relative magnitude Δm for the black hole with the mass $M = 60M_{\odot}$ is plotted but the curves with $M = 10M_{\odot}$ and $M = 30M_{\odot}$ are very similar to the one with $M = 60M_{\odot}$.

D. Retrolensing double image

We discuss a retrolensing double image with image angles θ_+ and θ_- by a charged black hole at $D_{OL} = 0.01\text{pc}$. From Eqs. (3.4) and (3.12), the separation $\theta_+ - \theta_-$ of the double image is given by

$$\theta_+ - \theta_- \sim 2\theta_+ = \theta_m \left[1 + \exp \left(\frac{\bar{b} - \pi + \beta}{\bar{a}} \right) \right]. \quad (3.16)$$

We define the relative separation $\Delta(\theta_+ - \theta_-)$ as the difference of the separation $\theta_+ - \theta_-$ of the double image retolensed by the charged black hole from the one by the non-charged black hole. Figures 10 and 11 show the separation $\theta_+ - \theta_-$ of the double image and the relative separation $\Delta(\theta_+ - \theta_-)$, respectively.

IV. DISCUSSION AND CONCLUSION

In this paper, we have obtained the deflection angle in the strong deflection limit analytically in the Reissner-Nordström spacetime while it could not be obtained in Ref. [17]. This is just because we have chosen a simple variable z (2.25). In Ref. [17] a variable $z_{[17]}$ defined by, in our notation,

$$z_{[17]} \equiv \frac{-g_{tt}(r) + g_{tt}(r_0)}{1 + g_{tt}(r_0)} \quad (4.1)$$

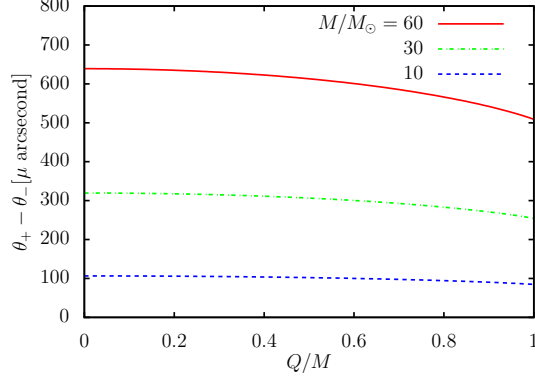


FIG. 10. Separation $\theta_+ - \theta_-$ of a double image as a function of Q/M . The (red) solid, (green) dash-dotted, and (blue) dashed curves denote the separation $\theta_+ - \theta_-$ of a double image lensed by black holes at $D_{OL} = 0.01\text{pc}$ with the mass $M = 60M_\odot$, $30M_\odot$, and $10M_\odot$, respectively.

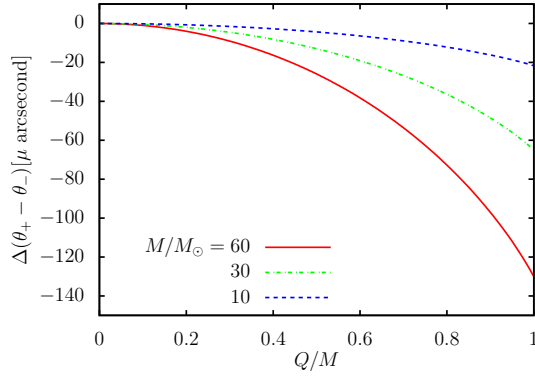


FIG. 11. Relative separation $\Delta(\theta_+ - \theta_-)$ as a function of Q/M . The (red) solid, (green) dash-dotted, and (blue) dashed curves denote the relative separation $\Delta(\theta_+ - \theta_-)$ by black holes at $D_{OL} = 0.01\text{pc}$ with the mass $M = 60M_\odot$, $30M_\odot$, and $10M_\odot$, respectively.

was used instead of z . See Eqs. (10) and (11) in [17]. Since $z_{[17]}$ in the Reissner-Nordström spacetime becomes

$$z_{[17]} = 1 - \frac{r_0^2 (2Mr - Q^2)}{r^2 (2Mr_0 - Q^2)}, \quad (4.2)$$

$z_{[17]}$ is not equivalent to z defined by Eq. (2.25). We also notice that $z_{[17]}$ is the same as z when the charge Q vanishes. Using the simple variable z (2.25), the deflection angle in the strong deflection limit in a general asymptotically flat, static, spherically symmetric spacetime will be developed in a follow-up publication [74].

Using the obtained deflection angle in the strong deflection limit in the Reissner-

Nordström spacetime, we have investigated retrolensing by a charged black hole near the solar system. We have shown that the effect of the electrical charge Q of the black hole on the magnitude of the light curves is small even if the black hole has the maximal electrical charge $Q = M$. The magnitude of the peak of the light curve depends on the reduced closest separation β_{min}/β_s between the center of the sun and the axis $\beta = 0$ on the source plane and one would estimate the reduced closest separation β_{min}/β_s from the characteristic shape of the peak of the light curve. Thus, unknown parameters of retrolensing are the distance between the observer and the black hole D_{OL} , the mass M and the electrical charge Q of the black hole.

We have also considered the separation of the double image which appears near outside the light sphere of the charged black hole. If the black hole has the maximal charge $Q = M$, the image separation is 20 percent smaller than the one by a non-charged black hole with the same mass. The image separations of retrolensing by a black hole with the mass $M = 10M_\odot$, $30M_\odot$, and $60M_\odot$ at $D_{OL} = 0.03\text{pc}$, 0.1pc , and 0.2pc , respectively, are $30\mu\text{arcsecond}$, which are the same size of the separation of the double image of light rays reflected by the light sphere of the black hole at center of our galaxy [15, 17]. If we are lucky, we can measure the image separation near outside the light sphere of a black hole passing by the solar system using near-future instrument.

If one believes that a non-rotating black hole should be described well by a Schwarzschild black hole, one can determine the mass M and its distance D_{OL} from the measurement of the image separation and the peak magnitude of the light curve. We have concentrated on retrolensing but if one also can measure another observable in a weak or strong gravitational field or the details of retrolensing, one can determine an additional parameter like Q or one can confirm that the lens object can be really regarded as the Schwarzschild black hole.

If one observes a light curve with precisely solar spectra on the ecliptic, one can say that it will be retrolensing caused by a light sphere as Holz and Wheeler pointed out [63]. The retrolens can be a black hole, a wormhole, or the other dark and compact objects with a light sphere and the observer will not distinguish them by the shapes of their retrolensing light curves since they will be very similar each other [60]. Even if one cannot detect any retrolensing light curves, one can give an upper bound of the number density of dark and compact objects with a light sphere from the observational data. In this paper, we have only considered a Reissner-Nordström black hole as a simple example but our conclusion

would not change much in the other non-rotating black hole spacetimes which include the Schwarzschild black hole spacetime as a special case. The consideration of the additional measurement of a black hole passing by the solar system without retrolensing and the further consideration of retrolensing by a Reissner-Nordström black hole and the other non-rotating black holes leave us future works.

ACKNOWLEDGEMENTS

NT thanks Ken-ichi Nakao, Tetsuya Shiromizu, Chul-Moon Yoo, and Takahisa Igata, for valuable comments. He also thanks Tomohiro Harada, Yoshimune Tomikawa, Hideki Asada, Hirotaka Yoshino, Yusuke Suzuki, Rio Saitou, and Takafumi Kokubu for useful conversations. This research was supported in part by the Natural Science Foundation of China under Grant No. 11475065 and the Program for New Century Excellent Talents in University under Grant No. NCET-12-0205.

-
- [1] P. Schneider, J. Ehlers, and E. E. Falco, *Gravitational Lenses* (Springer-Verlag, Berlin, 1992).
 - [2] A. O. Petters, H. Levine, and J. Wambsganss, *Singularity Theory and Gravitational Lensing* (Birkhauser, Boston, 2001).
 - [3] P. Schneider, C. S. Kochanek, and J. Wambsganss, *Gravitational Lensing: Strong, Weak and Micro, Lecture Notes of the 33rd Saas-Fee Advanced Course*, edited by G. Meylan, P. Jetzer, and P. North (Springer-Verlag, Berlin, 2006).
 - [4] M. Bartelmann, *Class. Quant. Grav.* **27**, 233001 (2010).
 - [5] V. Perlick, *Living Rev. Relativity* **7**, 9 (2004).
 - [6] V. Bozza, *Gen. Relativ. Gravit.* **42**, 2269 (2010).
 - [7] C. M. Claudel, K. S. Virbhadra, and G. F. R. Ellis, *J. Math. Phys.* **42**, 818 (2001).
 - [8] W. Hasse and V. Perlick, *Gen. Relativ. Gravit.* **34**, 415 (2002).
 - [9] C. Darwin, *Proc. R. Soc. Lond. A* **249** (1959).
 - [10] R. d' E. Atkinson, *Astron. J.* **70**, 517 (1965).
 - [11] J.-P. Luminet, *Astron. Astrophys.* **75**, 228 (1979).
 - [12] H. C. Ohanian, *Am. J. Phys.* **55**, 428 (1987).

- [13] R. J. Nemiroff, Am. J. Phys. **61**, 619 (1993).
- [14] S. Frittelli, T. P. Kling, and E. T. Newman, Phys. Rev. D **61**, 064021 (2000).
- [15] K. S. Virbhadra and G. F. R. Ellis, Phys. Rev. D **62**, 084003 (2000).
- [16] V. Bozza, S. Capozziello, G. Iovane, and G. Scarpetta, Gen. Relativ. Gravit. **33**, 1535 (2001).
- [17] V. Bozza, Phys. Rev. D **66**, 103001 (2002).
- [18] V. Perlick, Phys. Rev. D **69**, 064017 (2004).
- [19] S. V. Iyer and A. O. Petters, Gen. Rel. Grav. **39**, 1563 (2007).
- [20] V. Bozza and M. Sereno, Phys. Rev. D **73**, 103004 (2006).
- [21] V. Bozza and G. Scarpetta, Phys. Rev. D **76**, 083008 (2007).
- [22] V. Bozza, Phys. Rev. D **78**, 103005 (2008).
- [23] K. S. Virbhadra, Phys. Rev. D **79**, 083004 (2009).
- [24] A. Ishihara, Y. Suzuki, T. Ono, and H. Asada, arXiv:1612.04044 [gr-qc].
- [25] V. Bozza, Phys. Rev. D **67**, 103006 (2003).
- [26] E. F. Eiroa, G. E. Romero, and D. F. Torres, Phys. Rev. D **66**, 024010 (2002).
- [27] V. Bozza, F. De Luca, and G. Scarpetta, Phys. Rev. D **74**, 063001 (2006).
- [28] V. Bozza, F. De Luca, G. Scarpetta, and M. Sereno, Phys. Rev. D **72**, 083003 (2005).
- [29] H. Saida, arXiv:1606.04716 [astro-ph.HE].
- [30] S. Chen, S. Wang, Y. Huang, J. Jing, and S. Wang, arXiv:1611.08783 [gr-qc].
- [31] E. F. Eiroa, Phys. Rev. D **71**, 083010 (2005).
- [32] R. Whisker, Phys. Rev. D **71**, 064004 (2005).
- [33] E. F. Eiroa and C. M. Sendra, Phys. Rev. D **86**, 083009 (2012).
- [34] A. Bhadra, Phys. Rev. D **67**, 103009 (2003).
- [35] E. F. Eiroa, Phys. Rev. D **73**, 043002 (2006).
- [36] N. Mukherjee and A. S. Majumdar, Gen. Rel. Grav. **39**, 583 (2007).
- [37] G. N. Gyulchev and S. S. Yazadjiev, Phys. Rev. D **75**, 023006 (2007).
- [38] S. b. Chen and J. l. Jing, Phys. Rev. D **80**, 024036 (2009).
- [39] Y. Liu, S. Chen, and J. Jing, Phys. Rev. D **81**, 124017 (2010).
- [40] E. F. Eiroa and C. M. Sendra, Class. Quant. Grav. **28**, 085008 (2011).
- [41] C. Ding, S. Kang, C. Y. Chen, S. Chen, and J. Jing, Phys. Rev. D **83**, 084005 (2011).
- [42] S. Chen, Y. Liu, and J. Jing, Phys. Rev. D **83**, 124019 (2011).
- [43] S. W. Wei, Y. X. Liu, C. E. Fu, and K. Yang, JCAP **1210**, 053 (2012).

- [44] M. Azreg-Ainou, Phys. Rev. D **87**, 024012 (2013).
- [45] G. N. Gyulchev and I. Z. Stefanov, Phys. Rev. D **87**, 063005 (2013).
- [46] E. F. Eiroa and C. M. Sendra, Phys. Rev. D **88**, 103007 (2013).
- [47] S. W. Wei, K. Yang, and Y. X. Liu, Eur. Phys. J. C **75**, 253 (2015) Erratum: [Eur. Phys. J. C **75**, 331 (2015)].
- [48] E. F. Eiroa and C. M. Sendra, Eur. Phys. J. C **74**, 3171 (2014).
- [49] S. Sahu, K. Lochan, and D. Narasimha, Phys. Rev. D **91**, 063001 (2015).
- [50] H. Sotani and U. Miyamoto, Phys. Rev. D **92**, 044052 (2015).
- [51] S. S. Zhao and Y. Xie, JCAP **1607**, 007 (2016).
- [52] N. Tsukamoto, T. Kitamura, K. Nakajima, and H. Asada, Phys. Rev. D **90**, 064043 (2014).
- [53] K. S. Virbhadra and C. R. Keeton, Phys. Rev. D **77**, 124014 (2008).
- [54] K. S. Virbhadra and G. F. R. Ellis, Phys. Rev. D **65**, 103004 (2002).
- [55] T. K. Dey and S. Sen, Mod. Phys. Lett. A, **23**, 953 (2008).
- [56] K. K. Nandi, Y. Z. Zhang, and A. V. Zakharov, Phys. Rev. D **74**, 024020 (2006).
- [57] N. Tsukamoto, T. Harada, and K. Yajima, Phys. Rev. D **86**, 104062 (2012).
- [58] K. K. Nandi, A. A. Potapov, R. N. Izmailov, A. Tamang, and J. C. Evans, Phys. Rev. D **93**, no. 10, 104044 (2016).
- [59] N. Tsukamoto, Phys. Rev. D **94**, 124001 (2016).
- [60] N. Tsukamoto and T. Harada, arXiv:1607.01120 [gr-qc].
- [61] B. P. Abbott *et al.* [LIGO Scientific and Virgo Collaborations], Phys. Rev. Lett. **116**, 061102 (2016).
- [62] B. P. Abbott *et al.* [LIGO Scientific and Virgo Collaborations], Astrophys. J. **818**, L22 (2016).
- [63] D. E. Holz and J. A. Wheeler, Astrophys. J. **578**, 330 (2002).
- [64] E. F. Eiroa and D. F. Torres, Phys. Rev. D **69**, 063004 (2004).
- [65] V. Bozza and L. Mancini, Astrophys. J. **611**, 1045 (2004)
- [66] F. De Paolis, G. Ingrosso, A. Geralico, and A. A. Nucita, Astron. Astrophys. **409**, 809 (2003).
- [67] F. De Paolis, A. Geralico, G. Ingrosso, A. A. Nucita, and A. Qadir, Astron. Astrophys. **415**, 1 (2004).
- [68] I. Z. Stefanov, S. S. Yazadjiev, and G. G. Gyulchev, Phys. Rev. Lett. **104**, 251103 (2010).
- [69] S. W. Wei and Y. X. Liu, Phys. Rev. D **89**, 047502 (2014).
- [70] S. W. Wei, Y. X. Liu, and H. Guo, Phys. Rev. D **84**, 041501 (2011).

- [71] H. J. Witt and S. Mao, ApJ, **430**, 505 (1994).
- [72] R. J. Nemiroff and W. A. D. T. Wickramasinghe, Astrophys. J. **424**, L21 (1994).
- [73] C. Alcock *et al.* [MACHO and GMAN Collaborations], Astrophys. J. **491**, 436 (1997).
- [74] N. Tsukamoto, *Preprint* (2016).